Available online at www.sciencedirect.com
ScienceDirect
Bioorganic & Medicinal Chemistry Letters 18 (2008) 2701–2708
Bioorganic & Medicinal Chemistry Letters

A molecular modeling study of the interaction of 2′-fluoro-substituted analogues of dUMP/FdUMP with thymidylate synthase

Adam Jarmuła,* Anna Dowierciał and Wojciech Rode

Nencki Institute of Experimental Biology, Polish Academy of Sciences, Pasteura 3, 02-093 Warszawa, Poland

Received 8 January 2008; revised 3 March 2008; accepted 6 March 2008
Available online 10 March 2008

Abstract—Molecular dynamics simulations and free energy calculations are presented, exploring previously described experimentally studied interactions of a series of 2′-fluoro-substituted dUMP/FdUMP analogues with thymidylate synthase (TS). The results show the inhibitory behaviors of 2′-F-*ara*-UMP, 2′,2″-diF-dUMP and 2′,5-diF-*ara*-UMP to be dependent upon the binding positions and orientations adopted by the molecules of these compounds in the active site of TS. The binding mode of 2′,5-diF-*ara*-UMP suggests a novel role of the active site residue Trp 80, stabilizing through hydrophobic stacking the binding position of the pyrimidine ring in 2′,5-diF-*ara*-UMP.

Thymidylate synthase (TS) (EC 2.1.1.45) plays a central role in DNA synthesis. TS catalyzes the dUMP (2′-deoxyuridine-5′-monophosphate) methylation reaction involving a concerted transfer and the reduction of a single carbon (methylene) group of N^5,N^{10}-methylenetetrahydrofolate (mTHF), with concomitant production of dTMP (thymidylate monophosphate) and dihydrofolate (DHF).[1–3] The reaction has an ordered binding sequence, with dUMP binding at the active site before mTHF. The reaction is initiated by the nucleophilic addition of the active site Cys 146 (numbering of amino acid residues used in this paper is according to the sequence of *Escherichia coli* TS) to the pyrimidine C(6) atom of dUMP. Of special importance, at the start of catalysis, are the binding position and orientation of the substrate, which, if correctly adopted, support an efficient binding of the cofactor, thus allowing the formation of the ternary TS–dUMP–mTHF complex, and the subsequent reaction. TS accomplishes the correct positioning and orienting of its substrate by coordinating the molecule of dUMP via several hydrogen contacts. Among the most important are numerous H-bonds connecting certain arginine and serine residues of TS (Arg 21, Arg 166 and Ser 167 from one subunit, Arg 126′ and Arg 127′ from the other subunit of TS dimer) with the dUMP phosphate moiety, the latter acting as an anchor positioning the molecule of the substrate in the active site.[4] The hydrogen bonds between the O(4) atom and N(3)–H group of the uracil moiety of dUMP and Asn 177 are foremost essential in recognizing and orienting the substrate.[5,6] Other H-bonds connecting dUMP with TS, including that between the uracil O(2) atom and the amide nitrogen of Asp 169, as well as those between the deoxyribose 3′-hydroxyl group and the residues of His 207 and Tyr 209, are less important in positioning and/or orienting the substrate. However, the H-bond to uracil O(2) stabilizes the residue of Asp169 in an orientation from which its side chain hydrogen bonds directly to the pterin ring of the molecule of mTHF, thereby being supportive of a correct orientation of the cofactor upon the formation of the ternary complex.[7] On the other hand, the H-bonds to the 3′-hydroxyl group are not regarded as important for the binding process, as they are not sufficient to position the sugar moiety in the dUMP binding site in the absence of the pyrimidine ring.[2,4]

The reaction of TS is the sole intracellular source of de novo synthesized dTMP (one of the four building blocks of DNA). Inhibition of TS blocks DNA synthesis and prevents cellular proliferation. Therefore, targeting of TS for inactivation in TS-expressing tumor cells is an

Keywords: 2′-Fluoro-substituted dUMP/FdUMP analogues; Substrate-based inhibitors of thymidylate synthase; Thymidylate synthase; Molecular dynamics simulations; MM-GBSA approach.
* Corresponding author. Fax: +48 22 8225342; e-mail: a.jarmula@nencki.gov.pl

0960-894X/$ - see front matter © 2008 Elsevier Ltd. All rights reserved.
doi:10.1016/j.bmcl.2008.03.016

important strategy in developing drugs for cancer chemotherapy.[8,9] One of the potent TS inhibitors, a dUMP analogue 5-fluoro-dUMP (FdUMP) (Fig. 1),[10] is an active metabolite of a broadly used anticancer drug, 5-fluorouracil (5-FU).[11] The mechanism-based inhibition of TS by FdUMP involves a time-dependent formation of the ternary TS–FdUMP–mTHF complex, upon which the reaction stops as the fluorine substituent fails to dissociate from the pyrimidine ring, resulting in a slowly reversible inactivation of the enzyme.[12] 5-FU is not an optimal TS-inhibitory drug because it is inefficiently converted to FdUMP, with part of it catabolized to toxic metabolites. Moreover, tumors may exhibit acquired or intrinsic resistance to 5-FU.[13,14] Studies on the discovery of new effective and specific TS inhibitors or inhibitory strategies pertaining to the class of dUMP derivatives are in progress, with some of recent approaches focused on the substitutions at the C(5) and/or C(4) positions in the base of dUMP,[15–17] or on developing miscellaneous FdUMP or 5-FU pro-drugs or pro-drug strategies (ECTA) to overcome 5-FU resistance.[18–20]

Most recently, interaction with human recombinant thymidylate synthase of 2′-fluoro-substituted dUMP/FdUMP analogues was investigated.[21] Of the four analogues studied (Fig. 1), only 2′-F-dUMP (fluorine in the 'down' configuration) showed substrate activity, characterized by a K_m value of 12.2 μM, higher than that observed with dUMP (5.25 μM). Of the rest of analogues in the examined series, all three appeared to be competitive inhibitors versus dUMP. The apparent K_i^{app} values pointed to large differences between the affinities toward TS among the trio: from a strong interaction in the case of 2′,5-diF-*ara*-UMP (fluorine on C(2′) in the 'up' configuration; $K_i^{app} = 1.37$ μM) to a moderate one in the case of 2′-F-*ara*-UMP (fluorine 'up'; $K_i^{app} = 10.3$ μM) to an exceptionally weak one in the case of 2′,2″-diF-dUMP (fluorine both 'up' and 'down'; $K_i^{app} = 432.8$ μM). 2′-F-*ara*-UMP and 2′,2″-diF-dUMP were both classic inhibitors (no time dependence of inhibition observed), whereas 2′,5-diF-*ara*-UMP behaved as a slow-binding (time-dependent) inhibitor ($K_i = 4.77$ nM), apparently interacting with the enzyme in a way based on the mechanism of the reaction catalyzed by TS. Taken together, these results suggested the 2′-F substituent in the 'up' position to interfere with an initial attack of the TS Cys 146 on the pyrimidine C(6) atom of the nucleotide and the 5-F substituent to prevent this interference.

In order to explore and compare the binding behaviors of the 2′-fluoro-substituted dUMP/FdUMP analogues to TS and learn more about molecular aspects underlying the inhibitory actions of those analogues we undertook a series of molecular dynamics simulations (MDS). Owing to the lack of the crystal structure of human TS in binary complex with dUMP, the simulations were initiated from the crystal structure of the corresponding complex of *E. coli* TS with dUMP (PDB Accession Code 1bid).[4] Of note is that TS has a highly conservative sequence over most species. In particular, the active site composition, especially that in the dUMP binding site, is strongly preserved between human and *E. coli* thymidylate synthases.[22] Besides, the binding affinities of numerous individual dUMP analogues have been shown in the literature to exhibit a good qualitative correlation when measured against thymidylate synthases from different species, from bacterial to mammalian cells.[23] Therefore, it is justified to use the structure of *E. coli* TS in interpreting qualitatively the activity data measured in human TS.

Crystallographically refined water molecules were discarded. Hydrogen atom positions were built using the LEAP module of the AMBER 8 molecular modeling package.[24] The phosphate group in the nucleotides was kept deprotonated. Its charge of −2 was counterbalanced by the +1 charges on the two arginine residues (Arg 21 and Arg 166) hydrogen bonded to the phosphate. Substitutions in the dUMP molecule with the fluorine atom(s) resulted in the structures of the following complexes: TS–2′-F-*ara*-UMP, TS–2′,2″-diF-dUMP and TS–2′,5-diF-*ara*-UMP. Each structure was solvated in a truncated octahedron box of TIP3P water molecules,[25] with periodic boundary conditions. Sodium counterions were added to neutralize the net charge of the protein, bringing the total number of atoms in each system to 22157.

The partial atomic charges in the dUMP analogues were generated with the RESP method by fitting the electrostatic potentials calculated at the RHF/6-31G* level of theory.[26] MDS were performed using the SANDER module of AMBER 8. Energy minimizations using the steepest-descent and conjugate-gradient algorithms, followed by gradual heating to 300 K in three 7 ps intervals (0 K → 100 K, 100 K → 200 K, 200 K → 300 K), equilibrations at 300 K for 99 ps, and data production runs for 1000 ps, were carried out. The potential and kinetic energies of the modeled systems stabilized and started to oscillate about stable mean values around 50–60 ps. Therefore, neither equilibration phases longer than 99 ps nor data production runs longer than 1000 ps were arbitrated necessary to enhance the credibility and the accuracy of data. This was further confirmed by overall stable trajectories in the production phases of MDS (see Supplementary Data, Fig. 1S). The Duan et al. (ff03) force field was used.[27] Simulations were performed in the NpT ensemble with a constant temperature of 300 K and constant pressure of 1 atm. Temperature and pressure coupling parameters were both 1 ps. A 1 fs time step and the SHAKE algorithm to constrain hydrogen-heteroatom bonds were used.[28] An 8 Å atom-based cutoff for the summation of van der Waals interactions and the particle-mesh Ewald (PME) procedure to calculate long-range electrostatics were applied.[29] In AMBER 8, the reciprocal space Ewald sums are β-spline interpolated on a grid and the convolutions necessary to evaluate the sums are calculated via fast Fourier transforms. The density of the charge grid spacing used throughout the simulations was approximately 0.91 Å, and the charge grid was interpolated using a cubic β-spline of the order of 4 with the direct sum tolerance of 0.00001. Trajectory snapshots were saved every 1 ps, summing to a total of 1000 for each

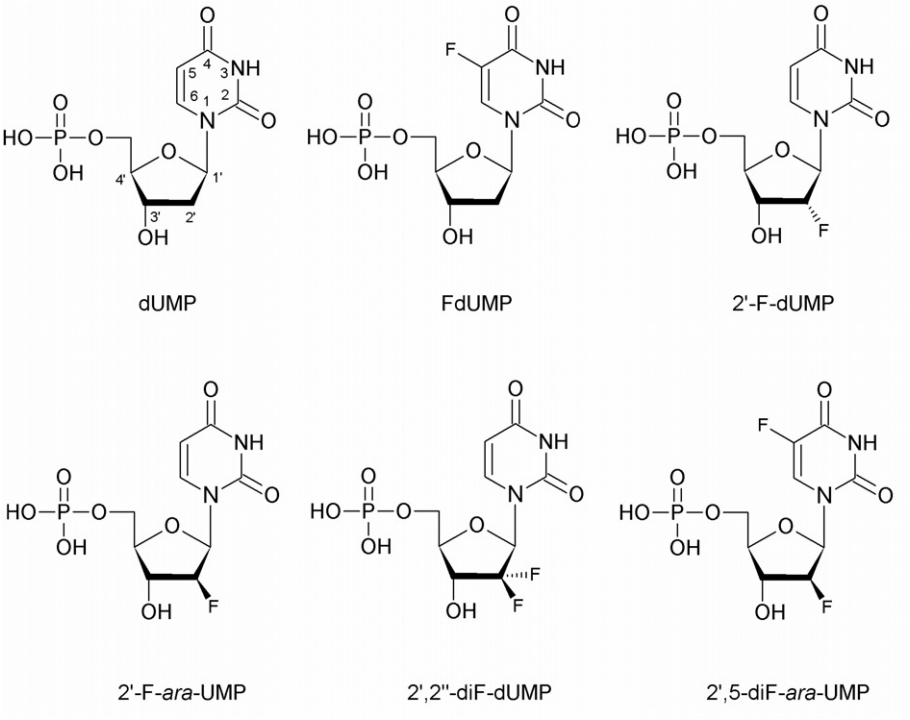

Figure 1. Schematic presentation of the structures of dUMP, FdUMP and their 2′-fluoro-substituted analogues. The atomic numbering is indicated in the structure of dUMP.

data production run. Average structures from the simulations, which are analyzed further in the article, were calculated by first stripping water and counterions and time-averaging the positions of the protein and ligand in the snapshots, and then briefly minimizing the average coordinates to ensure reasonable local geometry. To ascertain the statistical relevance of the average structures, detailed analysis of the trajectory snapshots was made. The RMSD of individual snapshots relative to the average structures were calculated (not shown), yielding moderate values in the range up to about 1.1 Å, on average about 0.65 Å. We verified that the conformational classes wherein the average structures belong were broadly populated in each phase of each corresponding molecular dynamics productive run, warranting that the conformational and structural information provided in the average structures was of relevance.

Based on the snapshots from the trajectories, relative free energies of binding of the 2′-fluoro-substituted dUMP/FdUMP analogues to TS were calculated using the MM-GBSA approach.[30] The binding free energy can be calculated according to the equation $\Delta G_{\text{bind}} = \Delta E_{\text{mm}} + \Delta G_{\text{solv}} - T\Delta S_{\text{solute}}$, where ΔE_{mm} is the molecular mechanics (MM) contribution to binding expressed as the sum of changes in the internal, electrostatic and van der Waals energies in the gas phase ($\Delta E_{\text{mm}} = \Delta E_{\text{int}} + \Delta E_{\text{ele}} + \Delta E_{\text{vdW}}$, respectively), ΔG_{solv} is the solvation free energy contribution to binding expressed as the sum of changes in the polar and non-polar solvation free energies ($\Delta G_{\text{solv}} = \Delta G_{\text{GB}} + \Delta G_{\text{np}}$, respectively), and $T\Delta S_{\text{solute}}$ is the contribution to binding from the change in the solute entropy. After discarding water and ion molecules, MM energies for the complex, receptor and ligand were calculated with SANDER using the infinite cutoff for all interactions and a dielectric constant of 1. Solvation free energies for the complex, receptor and ligand were calculated by applying a continuum representation of the solvent using the pairwise generalized Born (GB) model with the Tsui and Case parameters,[31–33] as implemented in SANDER. Dielectric constants of 1 and 80 were assigned to the solute and solvent, respectively. Atomic radii and charges were the same as used in explicit simulations. Non-polar solvation free energies for the complex, receptor and ligand were calculated based on solvent accessible surface area (SASA) with the LCPO method implemented in SANDER,[34] using the following equation: $G_{\text{np}} = \gamma\text{SASA} + b$, where $\gamma = 0.0072$ kcal/(mol Å^2) and $b = 0$ kcal/mol. The solute entropies were not calculated in this work assuming that the entropy changes would not contribute significantly to the relative binding free energies of structurally similar ligands to the same protein. Moreover, entropy calculation is very time-consuming for large systems and the normal mode analysis, which is often used to this task, usually offers only rough estimates with large margins of error.[35]

The root-mean-square deviations (RMSD) of the backbone atoms (N, C, CA, O) of the protein, relative to the coordinates of the crystal structure of the TS–dUMP complex, were calculated to assess the conformational stability of TS during the MDS courses. The values of 1.54, 1.67 and 1.78 Å, obtained for the complexes of TS with 2′,5-diF-*ara*-UMP, 2′-F-*ara*-UMP and 2′,2″-diF-dUMP, respectively, indicate a gradual change in the global conformation of the enzyme from the least (complex with 2′,5-diF-*ara*-UMP) to most (complex

with 2′,2″-diF-dUMP) different from the conformation present in the native TS–dUMP complex. Of note is that a negative correlation is apparent between the RMSD values and affinities toward TS exhibited by the compounds in the series (2′,5-diF-*ara*-UMP > 2′-F-*ara*-UMP > 2′,2″-diF-dUMP),[21] in accord with our earlier observation of departures from the structure of the native complex being associated with a reduced dUMP analogue–TS affinity.[36]

The molecules of 2′,5-diF-*ara*-UMP, 2′-F-*ara*-UMP and 2′,2″-diF-dUMP are in the *anti* sugar-base orientation in the average structures from MDS, with the glycosidic torsion angle belonging to the +*ap* (2′,5-diF-*ara*-UMP) or −*ac* (2′-F-*ara*-UMP and 2′,2″-diF-dUMP) range. The sugar puckering is C(2′)-*endo* in 2′,5-diF-*ara*-UMP, C(1′)-*exo*-O(4′)-*endo* in 2′-F-*ara*-UMP and C(1′)-*exo*-C(2′)-*endo* in 2′,2″-diF-dUMP. The average structures are shown superimposed on the crystal structure of the TS–dUMP complex (Fig. 2). The superimposition plots show significant differences between the positions of the molecules of 2′,5-diF-*ara*-UMP, 2′-F-*ara*-UMP and 2′,2″-diF-dUMP, relative to the position of the molecule of dUMP. The most conformity to the position of dUMP was found for the molecule of 2′,5-diF-*ara*-UMP, the pyrimidine ring of which is placed parallel to and oriented exactly the same as that of dUMP, maintaining important hydrogen contacts with surrounding TS residues (Table 1) and forming a solid binding surface for the mTHF cofactor molecule (Fig. 2a). Its position is stabilized, apart from the hydrogen bonds with Asn 177, and to a lesser extent Asp 169, via extensive stacking interactions with the indole ring of Trp 80, the latter residue being shifted from the position maintained in the TS–dUMP complex and placed parallel to the 2′,5-diF-*ara*-UMP pyrimidine ring, at a distance of about 3.5–4.0 Å. This stabilizing role of Trp 80 in the binding of 2′,5-diF-*ara*-UMP is a novel observation, as no specific role of Trp 80 in the binding of the substrate or its analogues has been so far reported. Of note is that holding its position as in the binary complex, Trp 80 would block the access, and thus prevent correct binding and alignment, of the cofactor molecule. However, superimposition of the structure of the TS–2′,5-diF-*ara*-UMP complex with the crystal structure of the ternary complex between *E. coli* TS, dUMP and tetrahydrofolate (THF) (PDB Accession Code 1kzi),[37] followed by a quick minimization, resulted in the THF molecule being placed close to parallel relative to the pyrimidine ring of 2′,5-diF-*ara*-UMP and well aligned for the catalysis (Fig. 3). This was possible, as Trp 80 slightly relocated, making room for the THF molecule. Moreover, having arrived at its new position, Trp 80 could stack with the pterin ring of THF, stabilizing the binding position of the cofactor. These results explain the behavior of 2′,5-diF-*ara*-UMP as a strong, mechanism-based inhibitor of TS.[21]

Each of the 2′-F-*ara*-UMP and dUMP molecules occupies the same binding site at the active site of TS, but orientations of the pyrimidine rings of both nucleotides differ by an angle of about 60° (Fig. 2b). It costs the 2′-F-*ara*-UMP uracil the loss of hydrogen bonds with Asn 177 (concerns only the O(4) atom, but not the N(3)–H group which is 'traced' by the amide carbonyl oxygen of Asn 177) and Asp 169, and of correct orientation of the C(6) atom with respect to the γS atom of the catalytic Cys 146, as well as some 0.6 Å increase in the C(6)–γS distance, from 3.16 Å in the TS–dUMP to 3.75 Å in the TS–2′-F-*ara*-UMP complex (Table 1). Trp 80 is shifted toward the pyrimidine ring of 2′-F-*ara*-UMP but, in contrast to the TS–2′,5-diF-*ara*-UMP complex, the overlapping between the indole ring of Trp 80 and the pyrimidine ring of 2′-F-*ara*-UMP is partial and the alignment quite far from parallel, so the stacking between the rings and the resulting stabilization effect are nearly absent. At last, the misalignment of the pyrimidine ring disturbs its ability to build the binding surface for and enable proper binding of the cofactor molecule (as concluded from the superimposition with the TS–dUMP–THF complex structure, not shown here). Together, these findings are in accord with 2′-F-*ara*-UMP lacking activity of a mechanism-based inhibitor of TS,[21] yet behaving as a classic inhibitor of moderate activity, competitive versus dUMP.

The 2′,2″-diF-dUMP molecule position shows by large the least conformity in the series with the position occupied by the molecule of dUMP. The pyrimidine rings in both molecules are not only separated from each other by a distance (measured between the centers of rings) of about 4.2 Å, but also show different orientations corresponding to about 60° angle rotation (Fig. 2c). The position of the pyrimidine ring of 2′,2″-diF-dUMP appears to result from its shift toward Trp 83. However, little stabilization is gained this way, as the overlapping between the 2′,2″-diF-dUMP pyrimidine and the Trp 83 indole ring is weak and the alignment significantly deviated from parallel, precluding the stacking plane-to-plane interactions, and allowing only a few hydrophobic contacts. Due to its altered position, the uracil moiety of 2′,2″-diF-dUMP loses the hydrogen contacts with Asn 177 and Asp 169 and the distance from C(6) to γS of Cys 146 distinctly increases, reaching 4.36 Å (Table 1). Coupled with γS facing away from the pyrimidine ring, the elongation of the C(6)–γS distance renders the approaching of γS to C(6) practically impossible, eliminating the possibility of a mechanism-based inhibition. Although dUMP and 2′,2″-diF-dUMP phosphate group positions essentially do not differ (even though the phosphate group of 2′,2″-diF-dUMP is lacking the H-bond with Arg 21, the loop of which has moved away from the active site), their deoxyribose moieties are in a distinct positional separation. Considering these positional differences and a low stabilization provided by the protein to the 2′,2″-diF-dUMP molecule at its binding site (most of the H-bonds mentioned in Table 1 are absent, with only a single compensating H-bond between O(4) and the hydroxyl of Tyr 94 present), it clearly appears why 2′,2″-diF-dUMP shows no real competition toward dUMP, with its low affinity to TS reflected by the K_i^{app} value, describing the inhibition of the TS reaction by this analogue, being exceptionally high (>0.4 mM).[21]

The present results show the 5-fluoro substitution in dUMP to counteract the effect of 2′-fluoro substitu-

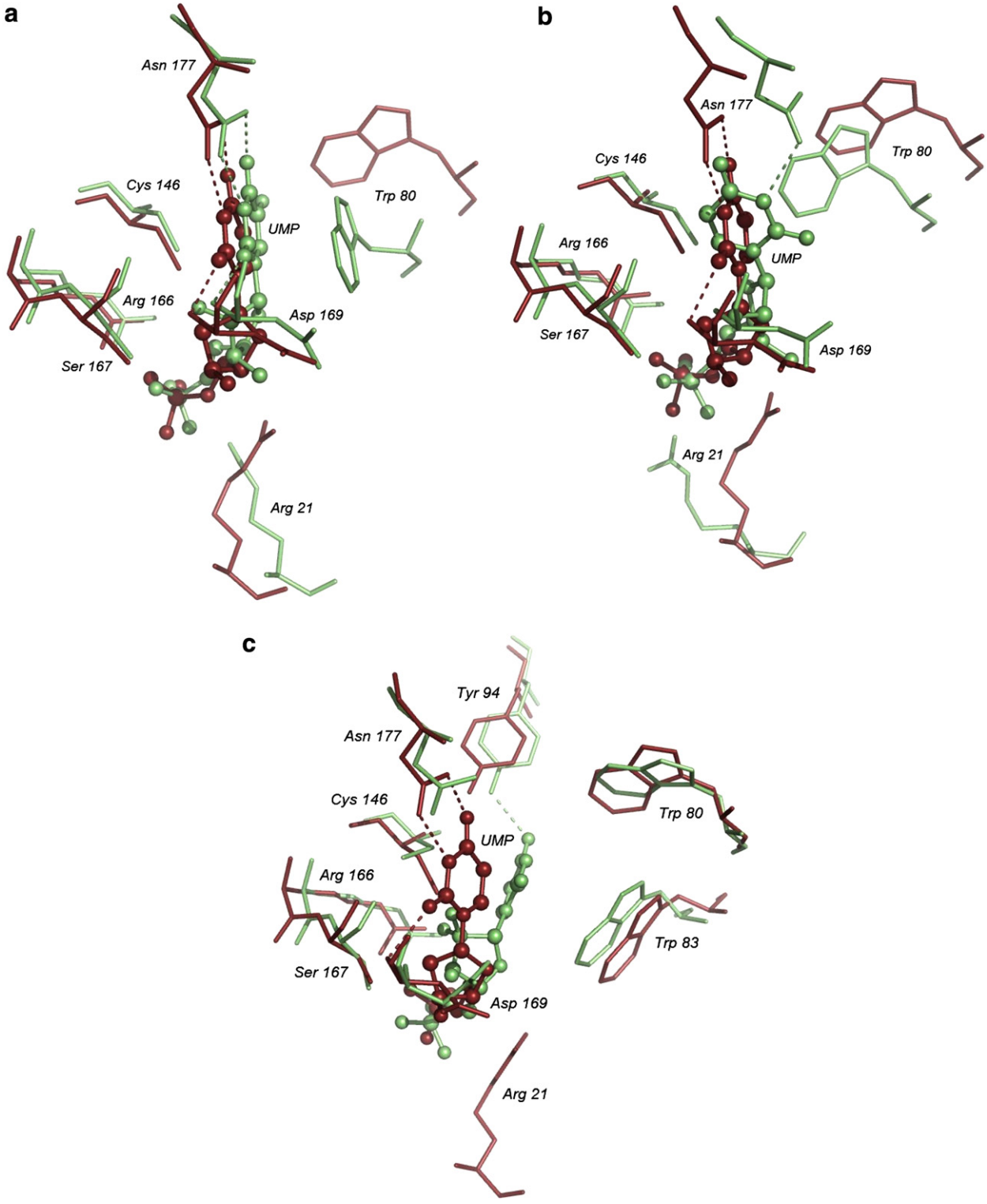

Figure 2. Superimposition plots of the average structures of the TS–2′,5-diF-*ara*-UMP [**2a**], TS–2′-F-*ara*-UMP [**2b**] and TS–2′,2″-diF-dUMP [**2c**] complexes (green) with the crystal structure of the TS–dUMP complex (red). Shown are amino acid residues that directly influence the binding of 2′,5-diF-*ara*-UMP, 2′-F-*ara*-UMP, 2′,2″-diF-dUMP and/or dUMP, and the catalytic Cys 146. The ligands (labeled as UMP) are shown in a ball-and-stick representation. H-bonds to the uracil ring in the ligands are indicated by dashed lines. Hydrogen atoms are omitted for clarity. This figure was prepared with PyMOL.[39]

tion by adjusting the sugar-base orientation from the *ac* (2′-F-*ara*-UMP and 2′,2″-diF-dUMP) to usual, highly populated among crystal structures of TS complexes with dUMP/dUMP analogues, *ap* range (2′,5-diF-*ara*-UMP). The latter adjustment supports proper orientation of the base of the 2′,5-diF-*ara*-UMP molecule, facilitating the nucleophilic addition of the catalytic Cys 146 to the pyrimidine ring, with the

Table 1. Distances [Å] between pyrimidine C(6) and γS of Cys 146 and the state of presence (+) or absence (−) of hydrogen bonds between dUMP (or its analogue) and TS

Complex	C(6)–γS distance	Hydrogen contacts with						
		Asn 177	Asp 169	His 207	Tyr 209	Arg 21[b]	Arg 166[b]	Ser 167
TS–dUMP (crystal)	3.16	+	+	+	+	+	+	+
TS–dUMP[a]	3.28	+	+	+	+	+	+	+
TS–FdUMP[a]	3.29	+	+	+	+	+	+	+
TS–2′,5-diF-*ara*-UMP	3.39	+	+	–	–	+	+	+
TS–2′-F-*ara*-UMP	3.75	+, –[c]	–	–	–	+	+	+
TS–2′,2″-diF-dUMP	4.36	–	–	–	–	–	+	+

[a] Data from Ref. 36.
[b] MDS were carried out in a single TS unit. Arg 126′ and Arg 127′ contributing to the phosphate-binding site from the other unit were not included.
[c] H-bond with uracil N(3)–H present, with O(4) absent.

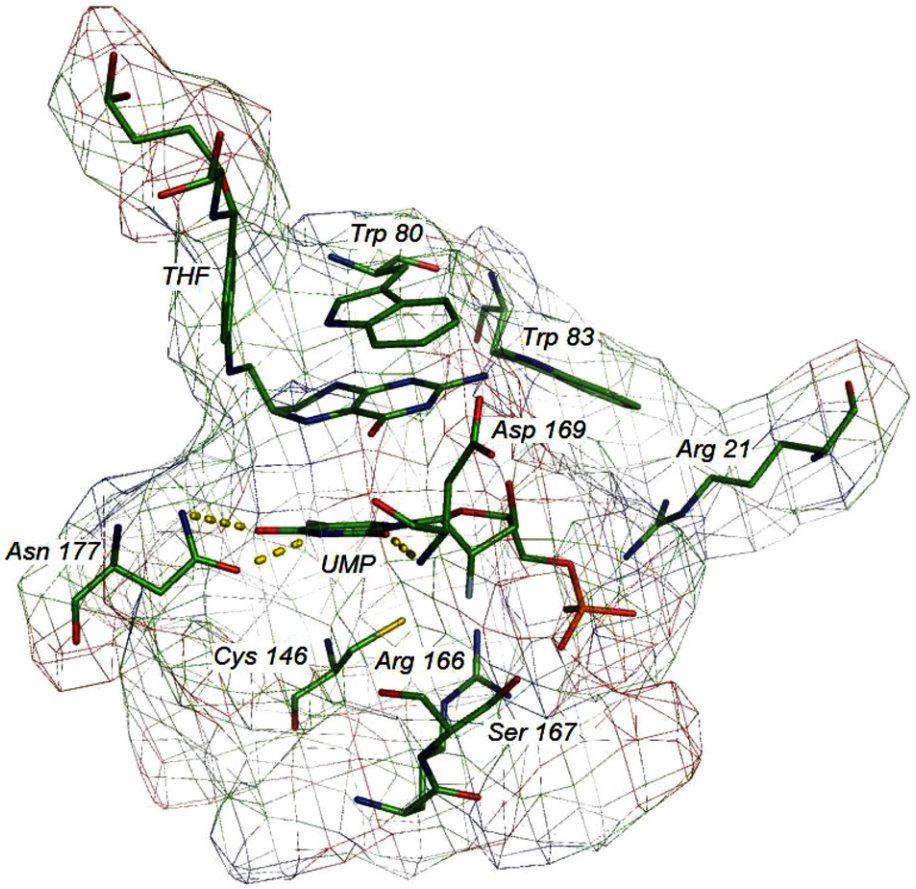

Figure 3. Superimposition plot of the average structure of the TS–2′,5-diF-*ara*-UMP complex with the crystal structure of the TS–dUMP–THF complex. Shown are the 2′,5-diF-*ara*-UMP (labeled as UMP) and THF molecules and important surrounding amino acid residues from the TS–2′,5-diF-*ara*-UMP complex. Carbon atoms are green, oxygen atoms are red, nitrogen atoms are dark blue, sulfur atom is yellow and phosphorus atom is orange. Hydrogen bonds to the uracil of 2′,5-diF-*ara*-UMP are marked as dashed lines. Hydrogen atoms are omitted for clarity. This figure was prepared with PyMOL.[39]

subsequent reaction of the mechanism-based inhibition. In the lack of the fluorine at C(5), the base of the 2′-F-*ara*-UMP molecule adopts wrong orientation, preventing the analogue from a mechanism-based reaction with TS.

Free energies of binding (ΔG_{bind} (calc)) were calculated both for the average structures analyzed in this paper and for the entire trajectories (Table 2). The values in Table 2 do not represent the absolute free energies since the entropy contribution to binding was not calculated. The ΔG_{bind} (calc) of the minimized average structures tend to be distinctly lower than the ΔG_{bind} (calc) calculated using the ensemble of fluctuating conformations collected in the trajectories, with both energies following the same rank order as the experimental free energies, estimated according to ΔG_{bind} (expt) $= -RT\ln(1/K_i^{app})$. The average structure ΔG_{bind} (calc) reflects very well

Table 2. Free energy results for the binding to TS of 2′,5-diF-*ara*-UMP, 2′-F-*ara*-UMP and 2′,2″-diF-dUMP

Complex	ΔG_{bind} (expt)	ΔE_{ele}	ΔE_{vdW}	ΔG_{GB}	ΔG_{np}	$\Delta G_{GB,ele}$[c]	ΔG_{bind} (calc)
Average structure calculation[a]							
TS–2′,5-diF-*ara*-UMP	−8.04	34.57	−25.77	−21.14	−4.70	13.43	−17.04
TS–2′-F-*ara*-UMP	−6.84	28.34	−19.77	−19.86	−4.49	8.48	−15.78
TS–2′,2″-diF-dUMP	−4.61	107.61	−20.12	−80.44	−3.97	27.17	3.08
Trajectory calculation[a,b]							
TS–2′,5-diF-*ara*-UMP	−8.04	137.24 (20.38)	−31.17 (3.68)	−96.69 (17.04)	−4.76 (0.13)	40.55 (5.46)	4.62 (4.71)
TS–2′-F-*ara*-UMP	−6.84	175.60 (21.95)	−27.05 (3.71)	−131.02 (18.18)	−4.89 (0.12)	44.58 (5.69)	12.64 (4.34)
TS–2′,2″-diF-dUMP	−4.61	228.81 (31.34)	−22.97 (3.22)	−180.74 (30.16)	−4.29 (0.20)	48.07 (4.98)	20.81 (4.33)

All energies are in kcal/mol.

[a] ΔE_{int} are not included as they amount to zero in the single trajectory approach.

[b] Averaged energies from 1000 snapshots from the trajectories (standard deviations in parentheses).

[c] $\Delta G_{GB,ele}$ is the sum of changes in the gas phase electrostatic energy and the polar solvation free energy, $\Delta E_{ele} + \Delta G_{GB}$.

the difference in ΔG_{bind} (expt) between the TS–2′,5-diF-*ara*-UMP and TS–2′-F-*ara*-UMP complexes (−1.26 vs −1.20 kcal/mol, respectively) while largely overestimating the ΔG_{bind} (expt) differences between the latter two and the TS–2′,2″-diF-dUMP complex (−20.12 and −18.86 vs −3.43 and −2.23 kcal/mol, respectively). The trajectory ΔG_{bind} (calc) occur at almost equal intervals of about 8 kcal/mol, noticeably overestimating the ΔG_{bind} (expt) differences between each two complexes. According to the contributions to the average structure ΔG_{bind} (calc), the most favorable ΔE_{vdW} is the main reason for the highest affinity to TS of 2′,5-diF-*ara*-UMP, while the strongly unfavorable $\Delta G_{GB,ele}$ disfavors the association with TS of 2′,2″-diF-dUMP. Components of the trajectory ΔG_{bind} (calc) show that the least unfavorable $\Delta G_{GB,ele}$ and the most favorable ΔE_{vdW} are primarily responsible for the highest affinity to TS of 2′,5-diF-*ara*-UMP, while the most unfavorable $\Delta G_{GB,ele}$ and the least favorable ΔE_{vdW}—for the lowest affinity of 2′,2″-diF-dUMP.

Together, the free energy results are in accord with the conclusions drawn from the analysis of the average structures from MDS. However, an unrealistically large difference in the ΔG_{bind} (calc) between the average structures of the TS–2′,5-diF-*ara*-UMP and TS–2′-F-*ara*-UMP complexes and the average structure of the TS–2′,2″-diF-dUMP complex suggests the latter structure may not represent quite well the real conformation of this complex. It seems possible that a true binding mode of a weakly binding 2′,2″-diF-dUMP may consist of several conformations, some of them being more favorable in terms of free energy than the conformation present in the average structure of the TS–2′,2″-diF-dUMP complex. While our MDS did not reveal any other major conformation than the latter one, it is possible that the hypothesized other conformations may populate different regions of the conformational space, that is, the ones inaccessible (in a reasonable time scale) to the simulations starting from the crystal structure of the TS–dUMP complex. Even if so, the main conclusion, linking a strongly reduced affinity for TS with a proposed shift in the binding position of 2′,2″-diF-dUMP, remains valid.

Our MDS results provide the molecular basis for understanding the competitive inhibitory behaviors of the 2′-fluoro-substituted dUMP/FdUMP analogues toward TS. Sharing the same binding position and orientation as dUMP was a prerequisite to a strong mechanism-based inhibition of TS by 2′,5-diF-*ara*-UMP. While differing in orientation, but preserving the binding site, was a condition for a modestly strong classic inhibition exhibited by 2′-F-*ara*-UMP, accommodating at a different binding site, weakly stabilized by TS, was a cause of a drastically lowered affinity for the enzyme shown by 2′,2″-diF-dUMP. We propose that beside its known roles in sequestering the reactants and stabilizing the cofactor cationic intermediate or transition state in the hydride transfer step of the TS catalytic mechanism,[37,38] the active site Trp 80 may also play a role in stabilizing, via favorable stacking interactions, the binding position of the pyrimidine ring in substrate analogues, as observed in the binding of 2′,5-diF-*ara*-UMP. Elucidating the roles of the active site residues may aid in developing rational approaches for inhibiting the TS reaction.

Acknowledgments

The computations were performed in part at the Interdisciplinary Centre for Mathematical and Computational Modeling of the Warsaw University (ICM).

Supplementary data

Supplementary data associated with this article can be found, in the online version, at doi:10.1016/j.bmcl.2008.03.016.

References and notes

1. Carreras, C. W.; Santi, D. V. *Annu. Rev. Biochem.* **1995**, *64*, 721.
2. Stroud, R. M.; Finer-Moore, J. S. *Biochemistry* **2003**, *42*, 239.
3. Finer-Moore, J. S.; Santi, D. V.; Stroud, R. M. *Biochemistry* **2003**, *42*, 248.

4. Stout, T. J.; Sage, C. R.; Stroud, R. M. *Structure* **1998**, *6*, 839.
5. Liu, L.; Santi, D. V. *Biochemistry* **1993**, *32*, 9263.
6. Finer-Moore, J. S.; Liu, L.; Schafmeister, C. E.; Birdsall, D. L.; Mau, T.; Santi, D. V.; Stroud, R. M. *Biochemistry* **1996**, *35*, 5125.
7. Sage, C. R.; Michelitsch, M. D.; Stout, T. J.; Biermann, D.; Nissen, R.; Finer-Moore, J.; Stroud, R. M. *Biochemistry* **1998**, *37*, 13893.
8. Chu, E.; Callender, M. A.; Farrell, M. P.; Schmitz, J. C. *Cancer Chemother. Pharmacol.* **2003**, *52*, S80.
9. Gmeiner, W. H. *Curr. Med. Chem.* **2005**, *12*, 191.
10. De Clercq, E.; Balzarini, J.; Torrence, P. F.; Mertes, M. P.; Schmidt, C. L.; Shugar, D.; Barr, P. J.; Jones, A. S.; Verhelst, G.; Walker, R. T. *Mol. Pharmacol.* **1981**, *19*, 321.
11. Grem, J. L. *Invest. New Drugs* **2000**, *18*, 299.
12. Santi, D. V.; McHenry, C. S.; Raines, R. T.; Ivanetich, K. M. *Biochemistry* **1987**, *26*, 8606.
13. Washtein, W. L. *Mol. Pharmacol.* **1984**, *25*, 171.
14. Berger, S. H.; Jenh, C. H.; Johnson, L. F.; Berger, F. G. *Mol. Pharmacol.* **1985**, *28*, 461.
15. Jarmuła, A.; Anulewicz, R.; Leś, A.; Cyrański, M. K.; Adamowicz, L.; Bretner, M.; Felczak, K.; Kulikowski, T.; Krygowski, T. M.; Rode, W. *Biochim. Biophys. Acta–Protein Struct. Mol. Enzymol.* **1998**, *1382*, 277.
16. Felczak, K.; Miazga, A.; Poznański, J.; Bretner, M.; Kulikowski, T.; Dzik, J. M.; Gołos, B.; Zieliński, Z.; Cieśla, J.; Rode, W. *J. Med. Chem.* **2000**, *43*, 4647.
17. Saxl, R. L.; Reston, J.; Nie, Z.; Kalman, T. I.; Maley, F. *Biochemistry* **2003**, *42*, 4544.
18. Bijnsdorp, I. V.; Comijn, E. M.; Padron, J. M.; Gmeiner, W. H.; Peters, G. J. *Oncol. Rep.* **2007**, *18*, 287.
19. Hoff, P. M. *Semin. Oncol.* **2003**, *30*, 88.
20. Lackey, D. B.; Groziak, M. P.; Sergeeva, M.; Beryt, M.; Boyer, C.; Stroud, R. M.; Sayre, P.; Park, J. W.; Johnston, P.; Slamon, D.; Shepard, H. M.; Pegram, M. *Biochem. Pharmacol.* **2001**, *61*, 179.
21. Ziemkowski, P.; Felczak, K.; Poznański, J.; Kulikowski, T.; Zieliński, Z.; Cieśla, J.; Rode, W. *Biochem. Biophys. Res. Commun.* **2007**, *362*, 37.
22. Almog, R.; Waddling, C. A.; Maley, F.; Maley, G. F.; Van Roey, P. *Protein Sci.* **2001**, *10*, 988.
23. Balzarini, J.; De Clercq, E.; Mertes, M. P.; Shugar, D.; Torrence, P. F. *Biochem. Pharmacol.* **1982**, *31*, 3673.
24. Case, D. A.; Darden, T. A.; Cheatham, T. E., III; Simmerling, C. L.; Wang, J.; Duke, R. E.; Luo, R.; Merz, K. M.; Wang, B.; Pearlman, D. A.; Crowley, M.; Brozell, S.; Tsui, V.; Gohlke, H.; Mongan, J.; Hornak, V.; Cui, G.; Beroza, P.; Schafmeister, C.; Caldwell, J. W.; Ross, W. S.; Kollman, P. A. AMBER 8. University of California: San Francisco, 2004.
25. Jorgensen, W. L. *J. Chem. Phys.* **1992**, *77*, 5757.
26. Bayly, C. I.; Cieplak, P.; Cornell, W. D.; Kollman, P. A. *J. Phys. Chem.* **1993**, *97*, 10269.
27. Duan, Y.; Wu, C.; Chowdhury, S.; Lee, M. C.; Xiong, G.; Zhang, W.; Yang, R.; Cieplak, P.; Luo, R.; Lee, T. *J. Comput. Chem.* **2003**, *24*, 1999.
28. Ryckaert, J. P.; Ciccotti, G.; Berendsen, H. J. C. *J. Comput. Phys.* **1977**, *23*, 327.
29. Essmann, U.; Perera, L.; Berkowitz, M. L.; Darden, T.; Lee, H.; Pedersen, L. G. *J. Chem. Phys.* **1995**, *103*, 8577.
30. Kollman, P. A.; Massova, I.; Reyes, C.; Kuhn, B.; Huo, S.; Chong, L.; Lee, M.; Lee, T.; Duan, Y.; Wang, W.; Donini, O.; Cieplak, P.; Srinivasan, J.; Case, D. A.; Cheatham, T. E., III *Acc. Chem. Res.* **2000**, *33*, 889.
31. Hawkins, G. D.; Cramer, C. J.; Truhlar, D. G. *Chem. Phys. Lett.* **1995**, *246*, 122.
32. Hawkins, G. D.; Cramer, C. J.; Truhlar, D. G. *J. Phys. Chem.* **1996**, *100*, 19824.
33. Tsui, V.; Case, D. A. *Biopolymers (Nucleic Acid Sci.)* **2001**, *56*, 275.
34. Weiser, J.; Shenkin, P. S.; Still, W. C. *J. Comput. Chem.* **1999**, *20*, 217.
35. Weis, A.; Katebzadeh, K.; Soderhjelm, P.; Nilsson, I.; Ryde, U. *J. Med. Chem.* **2006**, *49*, 6596.
36. Jarmuła, A.; Cieplak, P.; Krygowski, T. M.; Rode, W. *Bioorg. Med. Chem.* **2007**, *15*, 2346.
37. Fritz, T. A.; Liu, L.; Finer-Moore, J. S.; Stroud, R. M. *Biochemistry* **2002**, *41*, 7021.
38. Hong, B.; Haddad, M.; Maley, F.; Jensen, J. H.; Kohen, A. *J. Am. Chem. Soc.* **2006**, *128*, 5636.
39. DeLano, W. L. The PyMOL Molecular Graphics System. DeLano Scientific LLC: San Carlos, CA, USA. Available from: http://www.pymol.org.